# Double Ionization of Nitrogen from Multiple Orbitals

**Zhifeng Wu, Chengyin Wu,\* Xianrong Liu, Yongkai Deng, and Qihuang Gong\***

*State Key Laboratory for Mesoscopic Physics, Department of Physics, Peking University, Beijing 100871, People's Republic of China*

**Di Song and Hongmei Su\***

*State Key Laboratory of Molecular Reaction Dynamics, Beijing National Laboratory for Molecular Sciences (BNLMS), Institute of Chemistry, Chinese Academy of Sciences, Beijing 100190, People's Republic of China*

In intense femtosecond laser fields, molecules could be tunnel ionized from multiple valence orbitals, which produces molecular ions in different electronic states. In this article, we have used a reaction microscope to study double ionization of nitrogen by intense femtosecond laser pulses. It is found that some doubly charged molecular ions $N_2^{2+}$ are metastable while others dissociate through charge symmetric dissociation ($N_2^{2+} \rightarrow N^+ + N^+$) or charge asymmetric dissociation ($N_2^{2+} \rightarrow N^{2+} + N$). The kinetic energy releases and angular distributions of atomic ions are measured for the dissociation channels. With the aid of the CASSCF and MRCI calculations, the electronic states are identified and the contributions of the valence orbitals are discussed for these dissociated molecular dications.

## Introduction

The molecular dynamic behavior is significantly changed in the intense laser field.[1] When the laser intensity is above the ionization threshold of molecules, the external field asymmetrically distorts the potential energy surface and forms an exit potential barrier. In this case, tunneling ionization occurs and a singly charged molecular ion is formed. Until recently, only the highest occupied molecular orbital (HOMO) has been considered to explain the angular-dependent strong-field ionization and high harmonic generation (HHG) because of the exponential decay of the ionization rate on the electron binding energy.[2−7] On the basis of these measurements, molecular orbital and molecular structure are experimentally reconstructed.[5−7] However, recent works reveal that lower lying orbitals are involved in tunneling ionization of molecules through observing the alignment-dependent HHG emission or identifying the electronic state of the molecular ions.[8−11] Therefore, the contribution of these lower lying orbitals should be taken into consideration when molecular orbital or molecular structure is experimentally reconstructed.

When the laser intensity is further increased, several electrons are removed from molecules by such intense laser fields. Highly charged molecular ions are therefore formed. They will explode due to Coulomb repulsive force. Much attention has been focused on measuring the kinetic energy release (KER) from the Coulomb explosion of molecules with different charge states. The measurement indicates that Coulomb explosion occurs at a distance larger than the equilibrium distance of the corresponding neutral molecule if assuming that the KER comes from the potential energy of the Coulomb repulsion of the charges. This phenomenon has been well explained by charge resonance enhanced ionization, in which the ionization rate reaches a maximum at the critical internuclear distance.[12,13] Because it is very difficult to calculate, the actual potential energy curves

are always approximated by Coulomb potential curves for these highly charged molecular ions. Is this approximation accurate, especially for lower charge states? Doubly charged ions are the possible precursors of all higher charged molecules. Meanwhile, the potential energy curves of these doubly charged ions can be accurately calculated by using the CASSCF and MRCI method. With the aid of these theoretical calculations, it is now possible to deeply investigate the formation and decay routes of these doubly charged molecular ions. These studies are helpful to unravel the overall ionization dynamics for highly charged molecules.

Nitrogen is one of the most important ingredients of the atmosphere. The interaction between nitrogen and intense femtosecond laser has been studied extensively.[14−28] The tomographic reconstruction of the HOMO orbital is achieved by using high harmonics emission generated from intense femtosecond laser pulses focused on aligned nitrogen molecules.[5] The angular-dependent ionization probability is obtained through measuring the ion yield as a function of the angle between the laser polarization and the molecular axis.[6] Very recently, the contribution of the electrons occupying the HOMO-1 orbital has been identified for the laser-driven HHG.[10] Coulomb explosions of nitrogen are also extensively studied in intense laser pulses with different laser parameters. KERs are measured and explosion pathways are identified. The results show that multiple ionization occurs at larger internuclear distances and enhanced ionization dominates when the laser pulse durations are several tens or hundreds of femtoseconds. However, the internuclear distance is frozen near the equilibrium distance within the laser pulse duration for sub-10 fs laser pulses. Enhanced ionization is therefore greatly suppressed and multiple ionization occurs at short internuclear distances close to the neutral molecular equilibrium distances in the few-cycle laser field.[24]

In comparison with the single and multiple ionization of nitrogen, double ionization is scarcely studied. The influence of molecular structure on nonsequential double ionization has

\* To whom correspondence should be addressed. E-mail: cywu@pku.edu.cn, qhgong@pku.edu.cn, and hongmei@iccas.ac.cn.

been explored by measuring the momentum distributions of electrons produced in the double ionization of nitrogen.[29] Depending on the electronic states in which the doubly charged nitrogen ions are populated, parts of $N_2^{2+}$ are metastable, and others will dissociate through charge symmetric dissociation (CSD, $N_2^{2+} \rightarrow N^+ + N^+$) or charge asymmetric dissociation (CAD, $N_2^{2+} \rightarrow N^{2+} + N$).[16] Belerian and Cornaggia studied the dissociation temporal dynamics of these doubly charged nitrogen ions using a femtoscond pump−probe scheme based on Coulomb explosion imaging of the dissociating system.[30] Voss et al. observed that the KER has a structure for CSD with a high resolution kinetic energy release spectra.[21] Compared with the limited study of CSD, the study of CAD is even scarce for nitrogen in the intense infrared laser field. One of the reasons is that CAD is not easily observed when the laser pulse durations are longer than 40 fs.[24] Guo et al. observed the CAD of nitrogen with near-infrared 30 fs laser pulse for the first time.[16] The KER is 1.5 eV, much lower than that observed in previous experiments with soft X-ray radiation.[31] The authors proposed that the doubly charged nitrogen ion is created by a vertical ionization and the dissociation products are in excited electronic states. In this article, we study double ionization of nitrogen by intense femtosecond laser pulses using a reaction microscope. KER and angular distribution of atomic ions are measured for the excited doubly charged nitrogen that dissociates into $N^+ + N^+$ or $N^{2+} + N$. With the aid of ab initio calculations, we discuss the contribution of the valence orbitals for forming these excited molecular dications.

## Experimental Setup

The commercial laser system containing a Ti:sapphire oscillator and a multipass amplifier has been discussed elsewhere.[32,33] It delivers laser pulses with a central wavelength of 780 nm and pulse duration of 24 fs at a repetition rate of 3 kHz. The maximum pulse energy is 0.9 mJ and the laser polarization is horizontal. For the generation of a few-cycle pulse, the 24 fs laser pulse is further broadened in a 1 m hollow fiber filled with neon. The inner diameter of the fiber is 160 um. After collimation by an $f = 1$ m concave silver mirror, the laser is recompressed by five broadband chirped mirrors. In the beam path, two achromatic thin film polarizers with a thickness of 1.14 mm are used to attenuate the laser intensity. After dispersion compensation by another two broadband chirped mirrors, the pulse duration can be shortened to 8 fs before reaching the gas target. The incident laser is focused by a concave mirror with a focus length of 75 mm. The concave mirror is mounted on a three-dimensional manipulator inside the vacuum chamber. The laser intensity is calibrated by comparing the time-of-flight mass spectra of $H_2$ irradiated by intense laser pulses with previous reports.[34] The gaseous sample is diffused into the chamber continuously through a leak valve. The vapor pressure reaches $1 \times 10^{-9}$ mbar with a base pressure less than $1 \times 10^{-10}$ mbar. For the detection, we use coincident momentum imaging techniques. The signal is amplified by a MCP, with a position and time sensitive delay line detector (Roentdek DLD80) mounted on its back. The DLD signals are processed by an 8-channel multihit time-to-digital converter (CFD & TDC8HP) and stored on an event-by-event basis for off-line analysis. The position and flight time that the ions reach the detector are used to calculate momentum vectors of atomic ions with use of the Newton equation. KERs and angular distributions of these ions are further obtained from their momentum vectors. Because the leaked gas is a warm target, the initial velocity distribution of molecules is broad. The broad
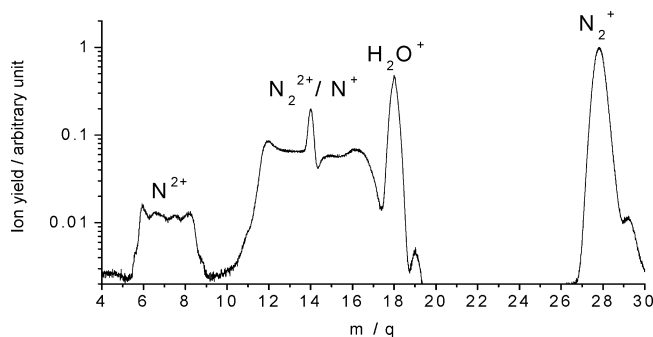


**Figure 1.** Time-of-flight mass spectra of $N_2$ irradiated by 24 fs, 780 nm, circularly polarized laser pulse at an intensity of $8 \times 10^{14}$ W/cm².
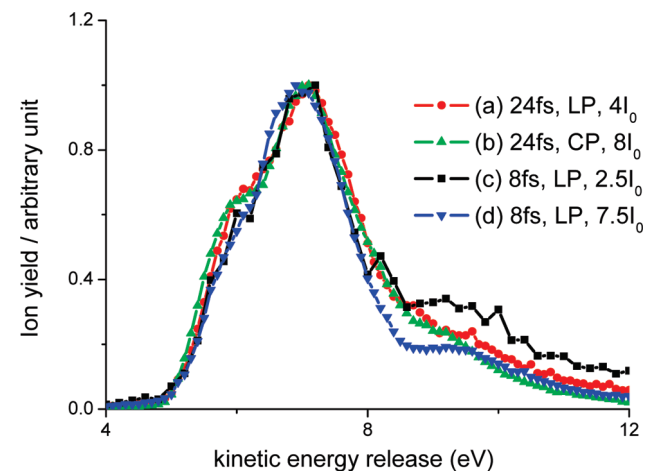


**Figure 2.** KER from the CSD of doubly charged nitrogen ions formed by (a) 24 fs, LP laser pulses at an intensity of $4.0I_0$, (b) 24 fs, CP laser pulses at an intensity of $8.0I_0$, (c) 8 fs, LP laser pulses at an intensity of $2.5I_0$, and (d) 8 fs, LP laser pulses at an intensity of $7.5I_0$ (LP: linearly polarized; CP: circularly polarized; $I_0$: $10^{14}$ W/cm²).

velocity distribution will limit the momentum resolution for the atomic ions produced in the CAD. However, the initial velocity distribution of molecules can be removed by using the "software cooling" program for the atomic ions produced in the CSD.[35,36] The concept of the "software cooling" method has been previously used to eliminate the Doppler broadening caused by the thermal motion of the parent molecules. Doppler-free high-resolution KER spectra are obtained by the coincident measurement of both fragmental ions generated in the dissociation of doubly charged molecules.[37]

## Results and Discussions

Figure 1 shows the time-of-flight mass spectra of $N_2$ irradiated by 24 fs, 780 nm circularly polarized laser pulses. The laser intensity is about $8 \times 10^{14}$ W/cm² and laser polarization is in the x−z plane. The z direction is along the time-of-flight mass spectrometer axis and the x−y plane is parallel to the MCP detector. A distinct crest is seen at m/q = 14 with flat distribution on both sides. The crest is composed of metastable $N_2^{2+}$ with a kinetic energy around zero. The excited states of doubly charged nitrogen ions are also populated, parts of them dissociate through CSD or CAD, and atomic ions are therefore generated.

Figure 2 shows the KER spectra from the CSD of doubly charged nitrogen ions, which are similar to previous reports.[20,21] These doubly charged nitrogen ions are formed by the interaction between neutral nitrogen molecules and femtosecond laser pulse with different pulse durations, polarizations, and intensi-

Double Ionization of Nitrogen from Multiple Orbitals

*J. Phys. Chem. A, Vol. 114, No. 25, 2010* **6753**

**TABLE 1: Electronic States of $N_2^{2+}$ with the Same Dissociation Limit $N^+(^3P) + N^+(^3P)$[a]**

| states | main electronic config | $T_0$ (eV) | KER (eV) | states | main electronic config | $T_0$ (eV) | KER (eV) |
|---|---|---|---|---|---|---|---|
| $1^1\Sigma_g^+$ | $3\sigma_g^{-2}$ | 42.60 | $-$[b] | $1^3\Pi_u$ | $1\pi_u^{-1}3\sigma_g^{-1}$ | 42.69 | $-$[b] |
| $1^1\Delta_g$ | $1\pi_u^{-2}3\sigma_g^{-0}$ | 44.09 | 7.79 | $1^3\Sigma_g^-$ | $1\pi_u^{-2}3\sigma_g^{-0}$ | 43.41 | 6.79 |
| $A^1\Pi_u$ | $1\pi_u^{-1}3\sigma_g^{-1}$ | 44.11 | 6.20 | $1^3\Sigma_u^+$ | $2\sigma_u^{-1}1\pi_u^{-0}3\sigma_g^{-1}$ | 44.10 | 5.22 |
| $2^1\Sigma_g^+$ | $1\pi_u^{-2}3\sigma_g^{-0}$ | 44.65 | 7.89 | $1^3\Pi_g$ | $2\sigma_u^{-1}1\pi_u^{-1}3\sigma_g^{-0}$ | 46.06 | 7.56 |
| $1^1\Pi_g$ | $2\sigma_u^{-1}1\pi_u^{-1}3\sigma_g^{-0}$ | 48.90 | 10.26 | $1^3\Delta_g$ | $-$ | | 11.96 |
| $1^1\Sigma_u^-$ | $-$ | | 14.41 | $2^3\Sigma_u^+$ | $-$ | | 13.04 |

[a] $T_0$ is the energy difference between the minimum of each potential energy curve and the ground state of the neutral nitrogen, KER is the energy difference between the energy of each potential energy curve at the equilibrium distance of the neutral nitrogen and the dissociation limit $N^+(^3P) + N^+(^3P)$. [b] Dissociation does not occur in the Franck–Condon region.
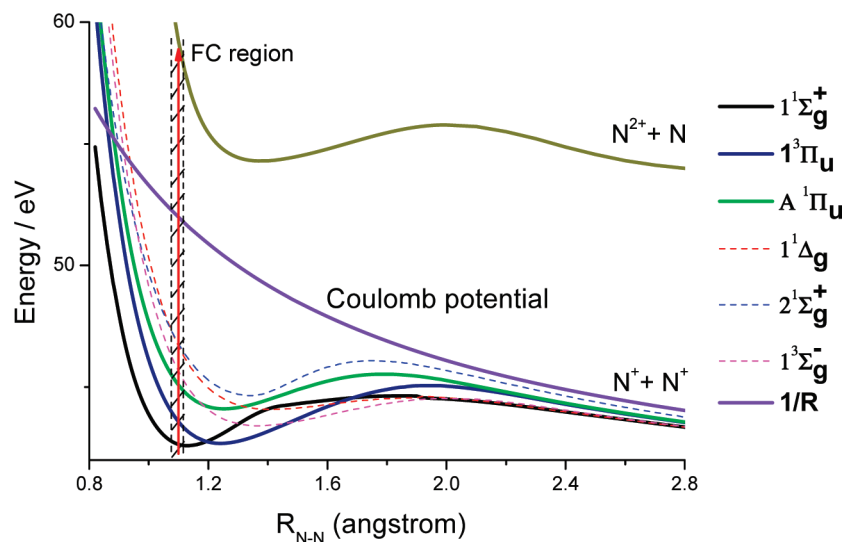


**Figure 3.** Potential energy curves of $N_2^{2+}$. Coulomb potential curve $(1/R)$ is also included for comparison.

ties. The KER spectra normalized with the peak height show that the spectra between 4 and 8 eV are similar for all the laser pulses irrespective of the pulse duration or the laser intensity. There are two obvious peaks. One is near 5.9 eV and the other is around 7.0 eV. The KER is far less than that from Coulomb potential curve $1/R$ at the equilibrium internuclear distance. The reduction of the KER should have nothing to do with the charge resonance enhanced ionization because enhanced ionization is greatly suppressed for nitrogen in the sub-10 fs laser field.[24] Most likely, the reduction is due to the strong presence of the bonding orbitals of the molecules. The CSD from some specific excited electronic states of $N_2^{2+}$ can lead to the KER spectra observed in the experiment.

To correlate the KER spectra with the electronic states, we calculate totally 15 electronic states of the species $N_2$, $N_2^+$, and $N_2^{2+}$. Table 1 lists 12 states of $N_2^{2+}$ associated with the products of $N^+(^3P_g) + N^+(^3P_g)$. The CASSCF and MRCI calculations at the level of the cc-pV5Z basis set are carried out with the MOLPRO Program package.[38] The MRCI are performed with a CASSCF wave function constituting the reference function. All valence electrons and orbitals are considered as active, while the $1\sigma_g$ and $1\sigma_u$ orbitals are doubly occupied in all calculations. In CASSCF calculation, the state-averaged method is used for the states which have $^1A_g$ and $^1B_u$ symmetries within the $D_{2h}$ subgroup, respectively. The final potential energy curves of these states are corrected in $D_{\infty h}$ symmetry.

Figure 3 shows the potential energy curves for those states relevant to the present study. When the doubly charged nitrogen ions are in the state of $1^1\Sigma_g^+$ or $1^3\Pi_u$, they are metastable assuming ionization dominates in the Franck–Condon region. They generate the peak at $m/q = 14$ in the time-of-flight mass spectra. From the major electronic configurations of these two

electronic states listed in Table 1, we know that they are formed through the removal of two electrons both in HOMO, or one in HOMO and the other in HOMO-1. The electronic state of $^1\Pi_u$ of $N_2^{2+}$ is a repulsive state if the internuclear distance does not change during the ionization process. The KER is calculated to be 6.2 eV when the dissociation occurs from this electronic state, which is consistent with the experimental value of 5.9 eV within the error bar. The electronic state of $^1\Pi_u$ of $N_2^{2+}$ is involved in the removal of two electrons, one from HOMO and the other from HOMO-1, while for the peak around 7.0 eV observed in the KER spectra, they might result from the dissociation of three electronic states, $^1\Delta_g$, $2^1\Sigma_g^+$, or $1^3\Sigma_g^-$. These electronic states are formed through the removal of two electrons both from HOMO-1.

The CAD of $N_2^{2+}$ is also observed in our experiment. However, it is a big challenge to calculate the potential energy curve of the CAD state of $N_2^{2+}$. The corresponding potential energy curve has not been reported yet. Recently, Franceschi et al. studied the production of the doubly charged ion $N^{2+}$ from $N_2$ using synchrotron radiation.[39] The appearance potential for $N^{2+}$ has been determined as $55.2 \pm 0.2$ eV, about 1.3 eV higher than the spectroscopic dissociation limit $N^{2+}(^2P) + N(^4S)$ at 53.9 eV. The results imply that the electronic state has a 1.3 eV potential barrier above the dissociation limit. Eberhardt et al. measured the energy-selected Auger electrons and the ions produced in the molecular fragmentation following core photoionization of $N_2$ with soft X-ray radiation.[31] They reported that the KER is $13.4 \pm 2$ eV when the binding energy is taken at 67 eV. The difference between the binding energy and the spectroscopic dissociation limit of $N^{2+}(^2P) + N(^4S)$ is 13.1 eV. The value is close to the KER measured in their experiment within the error bar. Thus, we speculate that the electronic state
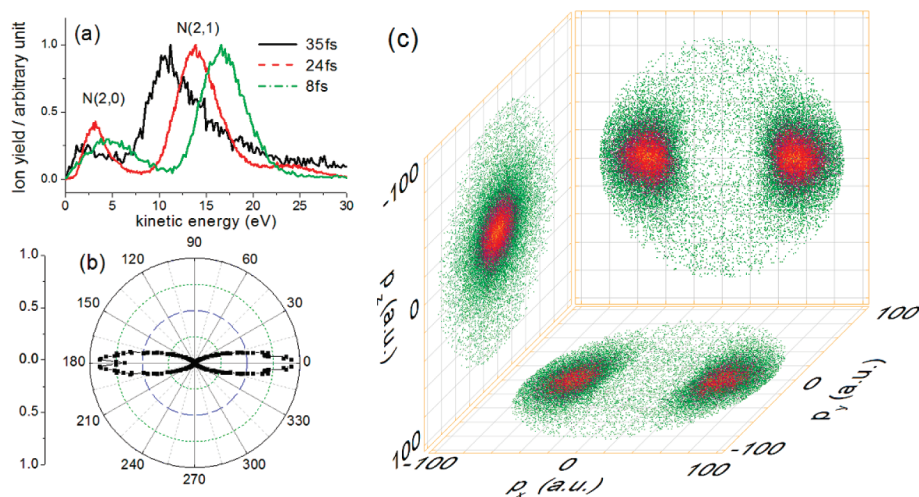
**Figure 4.** (a) KER from $N_2^{2+} \rightarrow N^{2+} + N$ (labeled as N(2,0)) and $N_2^{3+} \rightarrow N^{2+} + N^+$ (labeled as N(2,1)) formed by 35 fs, linearly polarized laser pulses at an intensity of $2.8I_0$ (black solid line), 24 fs, circularly polarized laser pulses at an intensity of $8.0I_0$ (red dash line), and 8 fs, circularly polarized laser pulses at an intensity of $10I_0$ (green dash dot line). (b) Angular distribution and (c) 3D momentum vectors of $N^{2+}$ produced in the CAD of doubly charged nitrogen ions formed by 24 fs, linearly polarized laser pulses at an intensity of $6.0I_0$. ($I_0$: $10^{14}$ W/cm$^2$.)

is the same for all these reports. This electronic state has a potential barrier of 1.3 eV higher than the spectroscopic dissociation limit $N^{2+}(^2P) + N(^4S)$. Even though CAD is studied with soft X-ray radiation,[31] synchrotron radiation,[39] and free-electron laser radiation,[40,41] the study of CAD with infrared field is scarce because this channel is not easily observed when the laser pulse durations are longer than 40 fs.[24] Guo et al.[16] first observed the CAD of nitrogen with near-infrared 30 fs laser pulse. The KER is 1.5 eV, much lower than that observed with soft X-ray radiation. The authors proposed that the doubly charged nitrogen is created while the internuclear distance does not change and the atomic fragments are in excited states.

We systematically study the CAD of nitrogen in intense femtosecond laser pulses with different laser parameters. The results show that the peak position of KER is mainly determined by the pulse durations. The KER spectra look alike independent of the laser polarization and the laser intensity when the pulse duration is fixed. However, the peak position of KER shifts toward lower energy with increasing the pulse duration. Figure 4a shows the KER for the CAD of nitrogen irradiated by intense laser pulses with different pulse durations. The peak positions of the KERs are around 1.6, 3.2, and 4.7 eV when the laser pulse durations are 35, 24, and 8 fs, respectively. Because of the presence of the CAD in circularly polarized laser fields, we conclude that the rescattering electron is not involved in forming the CAD state of $N_2^{2+}$. Since the appearance potential leading to CAD is very high, ionization of the inner valence electron should be involved. Theoretical calculation shows that the ionization contribution of the inner valence electron is small at lower laser intensity. However, the ionization probability for the inner-valence electron increases with increasing laser intensity.[42] The rising edge is different for the laser pulses with different pulse durations. The longer the pulse duration is, the longer the rising edge is. It is known that the internuclear distance will be stretched for molecules in intense laser fields according to the laser-assisted bond stretching model.[43] Long pulses allow more time for molecular stretching. The stretch of the internuclear distance results in the decrease of the KER with increased pulse duration.

The internuclear distance can be obtained through measuring the KER for a Coulomb explosion pathway because the KER mainly comes from the potential energy of the Coulomb

repulsion of the charges. To verify the stretch of the internuclear distance in intense laser fields, we also measure the KER from the Coulomb explosion pathway $N_2^{3+} \rightarrow N^{2+} + N^+$ channel (labeled as N(2,1)) with different pulse durations. The results are also included in Figure 4a. It can be seen that the KER shows a clear change toward low energy with increasing the pulse duration. This result verifies that the stretch degree of the internuclear distance is enhanced by increasing the pulse durations. The stretch of the internuclear distance can also explain the pulse duration effect on the appearance of CAD. For few-cycle laser pulses, nitrogen can experience a higher laser intensity before the internuclear distance is stretched due to the fast rising edge of the laser pulse. CAD is therefore easily observed, while for laser pulses with tens of femtoseconds pulse duration, internuclear distance will reach the critical distance before the transient laser field reaches the value for CAD. The dominant enhanced ionization will cover up CAD even though the maximum intensity is high enough. This might be the reason why the CAD channel of nitrogen is not easily observed when the laser pulse durations are longer than 40 fs.[24]

The potential energy curve is unavailable for the CAD state of $N_2^{2+}$ until now. Here, summarizing the present results and previous reports, we propose a sketch of the potential energy curve for the first time, which is shown in Figure 3. From the potential energy curve, we can see that a small stretch of the internuclear distance will lead to an obvious decrease of the KER of the CAD because the curve is steep near the equilibrium internuclear distance.

To identify the electron involved in the CAD, we also plot the angular distribution and three-dimensional momentum vectors of $N^{2+}$ produced in 24 fs, linearly polarized laser field with an intensity of $6 \times 10^{14}$ W/cm$^2$. The results are shown in Figure 4b,c. The maximum angular distribution and the momentum vectors of atomic ions are along the laser polarization. These observations indicate the involvement of $\sigma_g$ electron in forming the CAD state of doubly charged nitrogen ions. Considering the appearance potential of $55.2 \pm 0.2$ eV for this CAD channel,[39] we propose that the state involves the removal of one $2\sigma_g$ electron and one outer valence electron.

Double Ionization of Nitrogen from Multiple Orbitals

*J. Phys. Chem. A, Vol. 114, No. 25, 2010* **6755**

## Discussion: Ionization from Multiple Valence Orbitals

Tunneling ionization of molecules in intense laser fields creates a correlated electron wavepacket and a nuclear vibrational wavepacket of parent ion. In the oscillating laser fields, approximately half of the electron wavepacket and the parent ion severally reach the detector.[7] The remaining electron wavepacket is driven back to the parent ion. During the recollision process, laser-induced electron diffraction,[7] nonsequential double ionization,[20,29] and HHG[5] are observed. Because of the exponential decay of the ionization rate on the electron binding energy, only the HOMO orbital has been considered to explain these strong-field phenomena. These measurements are also used to image the HOMO orbital of the neutral molecule.[5] However, recent studies have shown that molecules could be tunnel ionized from multiple valence orbitals by measuring the alignment dependent HHG emission.[10,44] Unfortunately, sophisticated theories and some assumptions are required to identify the separate contributions of different valence orbitals to the HHG emission.[10,44] We know the tunneling ionization of molecules from different valence orbitals will leave the parent ion in different electronic states. For example, ionization from the HOMO of nitrogen will leave the nitrogen ion in the ground electronic state. Ionization from the HOMO-1 will leave the nitrogen ion in the first excited electronic state. Thus, tunneling current can be separated and identified by the coincident measurement with the parent ion in different electronic states.

Electron−electron correlation in double ionization of atom/molecule is a hot topic and has been extensively studied in recent years.[29] In these studies, the momentum distributions of electrons are measured irrespective of the electronic state of the parent ion.[29] However, double ionization is more complicated for molecules owing to the small energy separations and different geometries of valence orbitals. The present study demonstrates that double ionization of nitrogen occurs from multiple valence orbitals. The two electrons could be removed both from HOMO, or HOMO-1, or one from HOMO-1 and the other from HOMO. The separate contribution can be identified by the coincident measurement with the state-resolved molecular dications. These measurements could provide more precise information about electron−electron correlation in double ionization of molecules.

## Conclusions

Double ionization of nitrogen is experimentally studied with a reaction microscope. KER and momentum vectors are measured for CSD and CAD of doubly charged nitrogen ions. Features in the KER spectra reveal that some electronic states of the molecular dications are populated. With the aid of high-level ab initio calculation, we identify the CSD states of the molecular dications. These states are formed through removing two outer valence electrons. These two electrons are both from HOMO-1, or one from HOMO-1 and the other from HOMO, while for the CAD of doubly charged nitrogen ions, we found that the KER decreases with increasing the laser pulse duration. This phenomenon is explained by the stretch of the internuclear distance in intense laser fields. We also propose the potential energy curves of the CAD state of $N_2^{2+}$. This electronic state involves the removal of one $2\sigma_g$ electron and one outer valence electron.

## References and Notes

(1) Yamanouchi, K. *Science* **2002**, *295*, 1659.
(2) Guo, C. L. *Phys. Rev. Lett.* **2000**, *85*, 2276.
(3) Muth-Böhm, J.; Becker, A.; Faisal, F. H. M. *Phys. Rev. Lett.* **2000**, *85*, 2280.
(4) Tong, X. M.; Zhao, Z. X.; Lin, C. D. *Phys. Rev. A* **2002**, *66*, 033402.
(5) Itatani, J.; Levesque, J.; Zeidler, D.; Niikura, H.; Pépin, H.; Kieffer, J. C.; Corkum, P. B.; Villeneuve, D. M. *Nature (London)* **2004**, *432*, 867.
(6) Pavičič, D.; Lee, K. F.; Rayner, D. M.; Corkum, P. B.; Villeneuve, D. M. *Phys. Rev. Lett.* **2007**, *98*, 243001.
(7) Meckel, M.; Comtois, D.; Zeidler, D.; Staudte, A.; Pavičič, D.; Bandulet, H. C.; Pépin, H.; Kieffer, J. C.; Dörner, R.; Villeneuve, D. M.; Corkum, P. B. *Science* **2008**, *320*, 1478.
(8) Smirnova, O.; Mairesse, Y.; Patchkovskii, S.; Dudovich, N.; Villeneuve, D.; Corkum, P.; Ivanov, M. Y. *Nature (London)* **2009**, *460*, 972.
(9) Li, W.; Zhou, X.; Lock, R.; Patchkovskii, S.; Stolow, A.; Kapteyn, H. C.; Murnane, M. M. *Science* **2008**, *322*, 1207.
(10) McFarland, B. K.; Farrell, J. P.; Bucksbaum, P. H.; Gühr, M. *Science* **2008**, *322*, 1232.
(11) Akagi, H.; Otobe, T.; Staudte, A.; Shiner, A.; Turner, F.; Dörner, R.; Villeneuve, D. M.; Corkum, P. B. *Science* **2009**, *325*, 1364.
(12) Seideman, T.; Ivanov, M. Y.; Corkum, P. B. *Phys. Rev. Lett.* **1995**, *75*, 2819.
(13) Zuo, T.; Baudrauk, A. D. *Phys. Rev. A* **1995**, *52*, R2511.
(14) Cornaggia, C.; Lavancier, J.; Normand, D.; Morellec, J.; Liu, H. X. *Phys. Rev. A* **1990**, *42*, 5464.
(15) Hering, P.; Cornaggia, C. *Phys. Rev. A* **1998**, *57*, 4572.
(16) Guo, C. L.; Li, M.; Gibson, G. N. *Phys. Rev. Lett.* **1999**, *82*, 2492.
(17) Quaglia, L.; Cornaggia, C. *Phys. Rev. Lett.* **2000**, *84*, 4565.
(18) Wu, C.; Ren, H.; Liu, T.; Ma, R.; Yang, H.; Jiang, H.; Gong, Q. *Appl. Phys. B: Lasers Opt.* **2002**, *75*, 91.
(19) Nibarger, J. P.; Menon, S. V.; Gibson, G. N. *Phys. Rev. A* **2001**, *63*, 053406.
(20) Alnaser, A. S.; Voss, S.; Tong, X.-M.; Maharjan, C. M.; Ranitovic, P.; Ulrich, B.; Osipov, T.; Shan, B.; Chang, Z.; Cocke, C. L. *Phys. Rev. Lett.* **2004**, *93*, 113003.
(21) Voss, S.; Alnaser, A. S.; Tong, X. M.; Maharjan, C.; Ranitovic, P.; Ulrich, B.; Shan, B.; Chang, Z.; Lin, C. D.; Cocke, C. L. *J. Phys. B* **2004**, *37*, 4239.
(22) Coffee, R. N.; Gibson, G. N. *Phys. Rev. A* **2005**, *72*, 011401(R).
(23) Coffee, R. N.; Fang, L.; Gibson, G. N. *Phys. Rev. A* **2006**, *73*, 043417.
(24) Baldit, E.; Saugout, S.; Cornaggia, C. *Phys. Rev. A* **2005**, *71*, 021403(R).
(25) McKenna, J.; Suresh, M.; Srigengan, B.; Williams, I. D.; Bryan, W. A.; English, E. M. L.; Stebbings, S. L.; Newell, W. R.; Turcu, I. C. E.; Smith, J. M.; Divall, E. J.; Hooker, C. J.; Langley, A. J.; Collier, J. L. *Phys. Rev. A* **2006**, *73*, 043401.
(26) Liu, J.; Ye, D. F.; Chen, J.; Liu, X. *Phys. Rev. Lett.* **2007**, *99*, 013003.
(27) Guo, W.; Zhu, J. Y.; Wang, B. X.; Wang, Y. Q.; Wang, L. *Phys. Rev. A* **2008**, *77*, 033415.
(28) Plenge, J.; Wirsing, A.; Raschpichler, C.; Meyer, M.; Rühl, E. *J. Chem. Phys.* **2009**, *130*, 244313.
(29) Eremina, E.; Liu, X.; Rottke, H.; Sandner, W.; Schätzel, M. G.; Dreischuh, A.; Paulus, G. G.; Walther, H.; Moshammer, R.; Ullrich, J. *Phys. Rev. Lett.* **2004**, *92*, 173001.
(30) Beylerian, C.; Cornaggia, C. *J. Phys. B* **2004**, *37*, L259.
(31) Eberhardt, W.; Plummer, E. W.; Lyo, I.-W.; Carr, R.; Ford, W. K. *Phys. Rev. Lett.* **1987**, *58*, 207.
(32) Wu, Z.; Wu, C.; Liang, Q.; Wang, S.; Liu, M.; Deng, Y.; Gong, Q. *J. Chem. Phys.* **2007**, *126*, 074311.
(33) Wu, C.; Wu, Z.; Liang, Q.; Liu, M.; Deng, Y.; Gong, Q. *Phys. Rev. A* **2007**, *75*, 043408.
(34) Rudenko, A.; Feuerstein, B.; Zrost, K.; de Jesus, V. L. B.; Ergler, T.; Dimopoulou, C.; Schröter, C. D.; Moshammer, R.; Ullrich, J. *J. Phys. B* **2005**, *38*, 487.
(35) Liu, J.; Wu, J.; Czasch, A.; Zeng, H. *Opt. Express* **2009**, *17*, 12345.
(36) Wu, Z.; Wu, C.; Liu, X.; Liu, Y.; Deng, Y.; Gong, Q. *Opt. Express* **2010**, *18*, 10538.

(37) Lundqvist, M.; Baltzer, P.; Edvardsson, D.; Karlsson, L.; Wannberg, B. *Phy. Rev. Lett.* **1995**, *75*, 1058.

(38) MOLPRO, version 2009.1, a package of ab initio programs: Werner, H.-J.; Knowles, P. J.; Lindh, R.; Manby, F. R.; Schütz, M.; see http://www.molpro.net.

(39) Franceschi, P.; Ascenzi, D.; Tosi, P.; Thissen, R.; Žabka, J.; Roithová, J.; Ricketts, C. L.; Simone, M. D.; Coreno, M. *J. Chem. Phys.* **2007**, *126*, 134310.

(40) Jiang, Y. H.; Rudenko, A.; Kurka, M.; Kühnel, K. U.; Ergler, T.; Foucar, L.; Schöffler, M.; Schössler, S.; Havermeier, T.; Smolarski, M.; Cole, K.; Dörner, R.; Düsterer, S.; Treusch, R.; Gensch, M.; Schröter, C. D.; Moshammer, R.; Ullrich, J. *Phys. Rev. Lett.* **2009**, *102*, 123002.

(41) Fukuzawa, H.; Motomura, K.; Liu, X.-J.; Prümper, G.; Okunishi, M.; Ueda, K.; Saito, N.; Iwayama, H.; Nagaya, K.; Yao, M.; Nagasono, M.; Higashiya, A.; Yabashi, M.; Ishikawa, T.; Ohashi, H.; Kimura, H. *J. Phys. B* **2009**, *42*, 181001.

(42) Chu, X.; Chu, S.-I. *Phys. Rev. A* **2004**, *70*, 061402(R).

(43) Liang, Q.; Wu, C.; Wu, Z.; Liu, M.; Deng, Y.; Gong, Q. *Phys. Rev. A* **2009**, *79*, 045401.

(44) Haessler, S.; Caillat, J.; Boutu, W.; Giovanetti-Teixeira, C.; Ruchon, T.; Auguste, T.; Diveki, Z.; Breger, P.; Maquet, A.; Carre, B.; Taieb, R.; Salieres, P. *Nat. Phys.* **2010**, *6*, 200.